PAPER • **OPEN ACCESS**

Multi-resonant TVA formed by a tree of deflated composite beams with core structured fabrics

To cite this article: Paolo Gardonio *et al* 2025 *Smart Mater. Struct.* **34** 015039

OPEN ACCESS
IOP Publishing
Smart Materials and Structures
Smart Mater. Struct. **34** (2025) 015039 (14pp)
https://doi.org/10.1088/1361-665X/ad9c07

Multi-resonant TVA formed by a tree of deflated composite beams with core structured fabrics

Paolo Gardonio[1,*], Lisa Ortis[1], Emiliano Rustighi[2], Ciro Malacarne[3] and Matteo Perini[3]

[1] DPIA, University of Udine, Via delle Scienze 206, 33100 Udine, Italy
[2] DIE, University of Trento, Via Sommarive 9, 38123 Trento, Italy
[3] ProM Facility—Trentino Sviluppo S.p.A., Via Fortunato Zeni 8, 38068 Rovereto, TN, Italy

E-mail: paolo.gardonio@uniud.it

Received 22 August 2024, revised 4 December 2024
Accepted for publication 9 December 2024
Published 19 December 2024

Abstract

This paper presents a study on a multi-resonant tuneable vibration absorber for the control of flexural vibrations of thin structures in a low frequency band where the response is characterized by distinct lightly damped resonances of low order flexural modes. The absorber is formed by a tree of deflated composite beams made by a core structured fabric wrapped on a plastic skin. The beams have increasingly smaller length and are fixed in the middle on a mast that works as a base-post and vacuum-junction too. The fabric in each beam is made by a lattice of interlocked truss-like rigid particles. The uniform pressure exerted by the deflated skin forces the particles to jam such that the fabric moves from its natural fluid-like state to a solid state whose rigidity depends on the confining pressure exerted by the skin. Hence, each beam is characterized by a fundamental flapping vibration mode whose response resembles that of a classical mass-spring-damper vibration absorber and can be suitably tuned by adjusting the level of vacuum. The paper first analyses the working principles of single-beam and three-beams absorbers with respect to their vibration transmissibility and base impedance frequency response functions. Then, it presents the vibration control generated by the single-beam and the three-beams absorbers tuned to minimise the resonant responses of a single or three low order flexural modes of a thin plate. The paper shows that the operational frequency of each beam-absorber can be suitably adapted in a band of 8 Hz by varying the vacuum pressure in a 5–80 kPa range. Also, it shows that the single-beam or multi-beams absorbers reduce the resonant response of the target flexural modes by 10–20 dB.

Keywords: deflated adaptive element, tuneable vibration absorber, multi-resonant absorber, in-vacuo structured fabrics

* Author to whom any correspondence should be addressed.

1. Introduction

Structure-borne and air-borne noise transmission through lightweight structures is yet a relevant problem for the design of quite a vast range of mechanical systems, such as for example surface and air passenger transportation vehicles, domestic and professional appliances, machinery of production and processing factories, equipment of power plants, etc. The concurrent requirements for low fabrication and low exercise costs, as well as the need for a progressively lower ecological impact, have led to the design of increasingly lightweight structures and machineries that, indeed, warrant a lower exploitation of raw material and a lower consumption of energy during functioning. In general, the new generation of lightweight structures have a higher stiffness to mass ratio, which produces two effects on their vibration response and sound radiation. Firstly, the coincidence frequency between the flexural wavelength and the acoustic wavelength is shifted to lower frequencies [1] and, secondly, the low modal overlap frequency bandwidth of the flexural response is extended to higher frequencies [2, 3]. As a result, the low frequency band where the structure-borne and air-borne noise transmission is characterized by well separated resonant responses of low order lightly damped flexural modes is stretched towards higher frequencies. This leads to a net increment of both structure-borne and air-borne noise transmission in this extended low frequency band where, moreover, passive vibration control solutions are in general less effective unless heavy vibration (e.g. mass, stiffness, damping additions) and sound insulation (e.g. double wall constructions with porous liners) treatments are employed [4–6]. Controlling the resonant responses and sound radiation of lightly damped flexural modes with passive treatments is indeed a challenging task, both because they introduce significant weight penalties and because they cannot adapt to changes in the dynamic response of the structure generated by production (e.g. manufacturing repeatability) and operation conditions (e.g. wearing, temperature variations, imposed variable loads, etc). Starting from the 1980s, alternative solutions based on fully active or semi-active vibration control systems have been explored and developed [7–12]. Active systems are very appealing because they can generate significant vibration reductions, irrespectively the dynamic response of the structure may undergo large changes. Nevertheless, they are quite complex and costly systems, which have been adopted primarily in the transportation sector [13–15]. Semi-active vibration control systems are less complex [10, 12], and yet offer good control performances even in presence of a significant variability of the structural response. In this respect, quite a lot of work has been dedicated to the implementation of tuneable vibration absorbers (TVAs). These devices have been used quite extensively for about a century [16–19] and, as shown in classical textbooks [19–22], normally, they are made by a seismic mass fixed on an elastic suspension. To control the resonant response of a target flexural mode of a structure, the absorber should be mounted in an anti-nodal point. Also, its natural frequency should be tuned to about coincide with the natural frequency of the target mode and its damping should be set to maximize the vibration absorption by the absorber itself [3, 23]. Over the years quite a large bulk of studies were performed to find the laws for the optimal tuning of absorbers mounted on a simple resonant mechanical system [17–19, 24–31] These optimization studies have been extended with considerations on the time-history of real excitations [32, 33] and on the multi-resonant response of real flexible hosting structures [34, 35]. Besides, works were also presented on the control of multiple resonant responses of distributed structures using either multi-resonant vibration absorbers or multiple resonant absorbers [36–39]. Time-varying absorbers based on switching and sweeping concepts were also investigated to broaden their control frequency band [39–42]. In general, the tuning of the TVA damping factor is not so critical and, considering the mass of the absorber is normally 5% to 15% of that of the hosting structure, it should be comprised between 0.1 and 0.2. Instead, it is rather important that the TVA natural frequency, ω_a, is closely tuned to that of the resonant mode being controlled, ω_r (see formulae in [31]).

In practice, fixed tuning vibration absorbers can be successfully employed only in few cases where the resonant response of the hosting mechanical system can be accurately identified and does not change over time. As anticipated above, in most real applications, the dynamic response of the hosting system is affected by manufacturing variability and by wearing over time. Furthermore, it is likely to change significantly during operation due to temperature variations or imposed loads. In this case semi-active vibration absorbers should be employed, whose fundamental natural frequency and damping ratio can be tuned online to track the resonance frequency of the hosting structure target mode and to ensure the optimal damping is implemented [26, 43–48]. Over the years, several solutions have been studied encompassing magnetorheological elastomers [49, 50], shape memory alloys [51, 52], variable shape stiffness elements [53], shunted electromagnetic seismic transducers [31, 42, 54–59], piezoelectric seismic transducers [60, 61] and shunted piezoelectric patch strain transducers [62–67].

This paper proposes a new multi-resonant TVA, which can be adapted online to control multiple resonant responses of low order modes of a hosting structure subject to a broadband disturbance. The absorber is formed by a tree of deflated composite beams having increasingly smaller length. The beams are made by a core structured fabric wrapped on a plastic skin and are fastened on a centre mast that works as a base-post. The mast is designed in such a way as it provides independent vacuum junctions for all beams, which are connected via thin flexible tubes to a vacuum control plant. The fabric in each beam is made in plastic with 3D-printing and is composed by a regular network of interlocked hollowed truss-like rigid particles [68, 69], which resembles the medieval chain armours [70, 71]. The uniform pressure generated by the deflated plastic skin forces the particles to jam [72–78] such that the coated fabric becomes a solid body whose stiffness progressively increases as the vacuum pressure is raised [68, 69]. The hollowed truss-like particles of the structured fabrics

develop contacts between convex surfaces and between non-convex surfaces of the particles, which, for simplicity, will be referred to as convex and non-convex contacts hereafter [78–80]. Like with solid granular materials [81], the convex contacts produce significant normal-compressive resistance [82–84] and, according to [68], the non-convex contacts generate significant normal-tensile resistance. As shown in [68, 69], the combination of the compressive and tensile resistance effects leads to substantial bending resistance even in thin in-vacuo composite structures made with a single chain mail fabric. Overall, each beam of the multi-resonant vibration absorber displays a fundamental flapping vibration mode whose dynamic response resembles that of classical mass-spring-damper absorbers with tuneable fundamental resonance frequency [85, 86]. In this respect, [86] showed that, with vacuum pressures comprised between 5 and 80 kPa the convex and non-convex contacts that develop between the particles of the fabric can lead to rather high increments of the bending stiffnesses of the flapping beams such that their fundamental resonance frequencies can be shifted by 10% or more depending on the number of fabrics piled in the deflated bag and the type, geometry and material of the particles of the fabrics themselves. The length of the beams is chosen such that each element in the tree resonates at the nominal resonance frequency of a target flexural mode of the hosting structure. The exact tuning is then implemented online by varying the level of vacuum in each composite beam. In this way the absorber will work regardless the dynamics of the hosting structure may differ from the nominal value because of manufacturing variability or wearing over time. Also, during operation, it will adapt to changes that may arise in the dynamic response of both the hosting structure and the absorber itself, caused for example by temperature variations or imposed loads. The self-tuning function will require a vacuum controller, which should be set to maximise the vibration energy absorption by the TVA [23]. This paper is focussed on the physics of the absorber; thus, the vacuum was controlled manually with a trial-and-error approach.

The paper is structured in five parts. To start with, section 2 describes the proposed multi-resonant TVA and the vacuum plant developed to control the level of vacuum in each composite beam of the absorber. Then, section 3 presents a comprehensive analysis of the TVA vibration response. For simplicity, to start with, the response of a device with a single beam is investigated with respect to (a) the vibration transmissibility frequency response functions (FRFs) between the displacements at the base and tips of the beam element and (b) the mechanical base impedance FRF. Then, the base impedance FRF of a multi-resonant absorber encompassing a stack of three composite beams is examined. Following, section 4 presents a comprehensive analysis of the vibration control effects generated on the global flexural response of a thin plate model structure excited by a broad-band white noise force. To start with, the vibration control effects produced by a single-resonant TVA are investigated when the absorber is tuned to control in turn the first, second and fourth resonant responses of the plate (the third one is rather low and thus was not controlled). Then the control performance of a multi-resonant TVA formed by a pile of three composite beams tuned to control simultaneously the three resonant responses of the plate is examined in detail. Finally, section 5 reports the conclusions of the study.

2. Multi-resonant TVA

The design of the multi-resonant absorber encompassing a tree of deflated composite beams is first revised in this section together with the vacuum control plant, which was assembled from off-the-shelf components.

2.1. Tree of deflated composite beams

As shown in figure 1(a), the multi-resonant TVA presented in this study is formed by a stack of three beam-like composite structures having progressively smaller length. These elements are held together by a centre mast formed by the posts shown by the magnified figure 1(b). As depicted in figures 2(a) and (b), each composite beam is made by a core layer of interlocked rigid truss-like hollowed particles with spherical-octahedral shape [69], which is wrapped on a sealed plastic skin. As highlighted in figure 1(b), the bottom skin of each composite beam is fastened and sealed with butyl tape on a junction component, that works as vacuum inlet element too.

Without the outer skin, the chain mail fabric shows a fluid-like state due to the mobility of the loosely interlocked grains (figure 2(a)). However, when the fabric is encased in a deflated bag, the uniform pressure exerted by the plastic skin forces the truss-like hollowed grains to jam and lock such that the whole composite beam becomes solid (figure 2(b)) [72–78]. As discussed in [68]. (see page 241—graph 3(c), (d)), unlike conventional granular materials, the jamming of the truss-like hollowed particles is characterized by both convex and non-convex contacts [78–80]. At the grains scale, both types of contacts result in a compressive friction phenomenon [72–74]. However, at the larger scale of the composite beam, the convex and non-convex contacts generate resistances to compression and to traction respectively [68], which are essential to develop a resistance to bending. In this respect, [69] showed with four-point bending tests that the bending stiffness of a beam-like specimen encompassing the structured fabric with spherical-octahedral grains can be increased by about 40% by raising the vacuum pressure from 20 kPa to 80 kPa. Furthermore, the study presented in [86] showed that when the same specimen is held in the middle, the flexural response induced by the base post vibrations is characterised by a flapping fundamental mode whose resonance frequency can be raised by about 20% when the vacuum pressure is brought up from 5 kPa to 80 kPa.

The deflated beam elements in the TVA are designed with respect to the middle value of the vacuum working range ΔP, which in this study is comprised between 5 and 80 kPa. In this way, the resonance frequency of each element can be

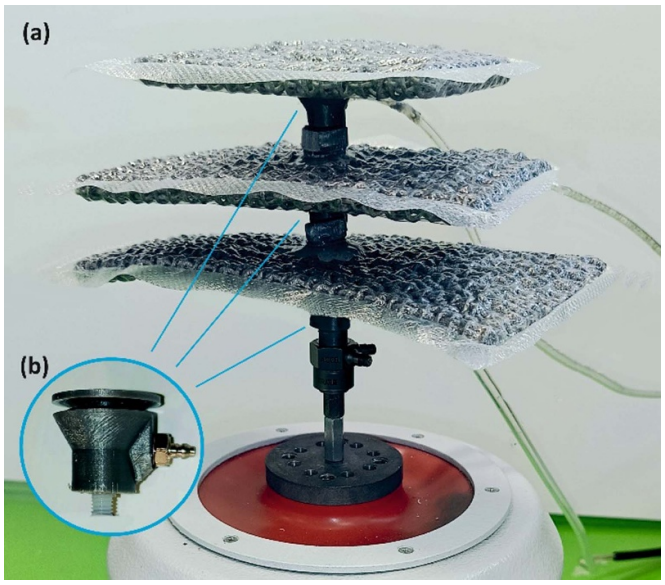

Figure 1. (a) Multi-resonant vibration absorber formed by a stack of three composite beams made by a core fabric wrapped on a deflated plastic skin. (b) Post vacuum junction.

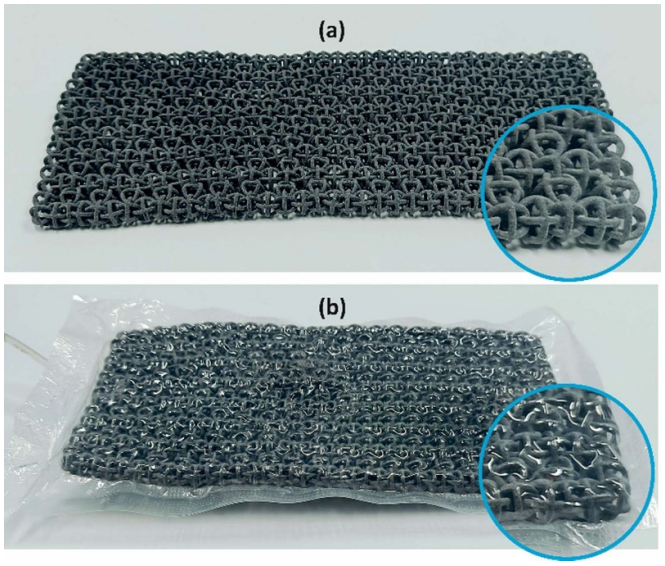

Figure 2. (a) Core fabric made of spherical-octahedral particles. (b) Core fabric wrapped on a deflated plastic skin.

equally raised or lowered by $\Delta\omega/2$, where $\Delta\omega$ is the tuning frequency band allowed by the ΔP vacuum range. More specifically, recalling that the natural frequency of the optimally tuned absorber should be set close to the natural frequency of the controlled mode of the hosting structure (e.g. see [31]), each element is set to resonate at the nominal resonance frequency of a target bending mode of the host structure. Exact tuning is then achieved online by adapting the vacuum level in each beam element. In this way the absorber will be adjusted to the exact dynamic-response of the host structure, which may differ due to production variability or due to wearing over time. Furthermore, during operation, it will adapt in real time to changes of its dynamic response and of the flexural response of the host structure, which can be generated by temperature variations or imposed workloads. In practice the beam elements are designed as if they were clamped in the middle section such that the natural frequency of the flapping vibration mode is given by the fundamental natural frequency of a half span cantilever beam element, which, according to [87], is given by

$$\omega_1 = \frac{4\lambda_1^2}{L^2}\sqrt{\frac{B}{m}}. \tag{1}$$

Here $\lambda_1 = 1.875$, L is the length of the whole beam, B is the bending stiffness and m is the mass per unit length of the beam. The bending stiffness cannot be predicted with classical formulae of solid mechanics, but, as shown in [69], it can be measured with 4 points bending tests at given values of vacuum pressure. The mass per unit length can equally be retrieved from measurements taken on the specimens at given values of vacuum pressure. As mentioned above, the damping generated by the absorber does not need fine tuning and thus was fixed upfront. The experiments presented in [86] showed that the flapping vibration of the composite beam elements generate about 20% damping ratio, which would ensure a correct functioning of the absorber.

2.2. *Vacuum plant*

As discussed above, the bending stiffness, and thus the fundamental resonance frequency, of the composite beams forming the multi-resonant TVA can be conveniently adapted by varying the level of vacuum in the encasing bag. For this study, the vacuum plant shown in figure 3(a) was devised and built using off-the-shelf components. According to figure 3(b), the plant is conceived around a vessel whose vacuum pressure is kept to a low value with a vacuum pump controlled by a pressure switch and a valve. The vessel is then equipped with a network of tubes encompassing a check valve, three vacuum valves and a release valve. The release valve is used to inflate the composite beams of the TVA up to ambient pressure. Hence, the system does not consider the pressurization of the composite beams themselves. To deflate the composite beams, the check and vacuum valves are opened whereas the release valve is shut. Alternatively, to inflate the composite beams the check valve is shut and the release and vacuum valves are opened. To avoid the vacuum pump and the deflated composite beams are connected simultaneously to the vessel, the check valve is also shut when the pump is activated by the pressure switch. A pressure gauge is insert in the network of vacuum tubes to monitor and control the vacuum pressure in the composite beams of the multi-resonant TVA.

The check, vacuum and release valves, as well as the vacuum gauge, are connected to a digital controller for the online control of the vacuum pressure in the three composite beams of the multi-resonant absorber. In this way the fundamental resonance frequencies of the three flapping beams, that is of the three absorbers forming the multi-resonant TVA,

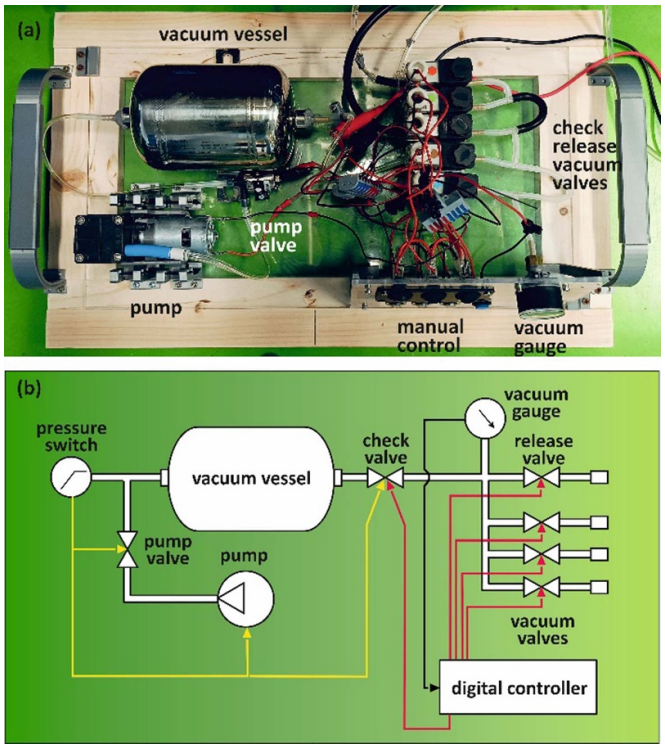

Figure 3. Vacuum plant. (a) Photo of the rig assembled from off-the-shelf components. (b) Working scheme.

can be conveniently tuned in such a way as to control the resonant responses of target modes. For instance, this can be done online by setting the multi-mode absorber to maximize the vibration power absorption from the hosting system [23], which can be conveniently measured with a load cell and an accelerometer at the base of the mast with the pile of three flapping beams. In this respect the tuning can be implemented online using the model free extremum seeking algorithm [67]. However, the focus of this paper is on the physics of the proposed multi-resonant vibration absorber, hence the tuning of each deflated beam absorber was done manually with a trial-and-error procedure.

3. TVA vibration response identification

The vibration response of the multi-resonant TVA is now investigated in two steps. Firstly, as depicted in figure 4(a), the response of a single-resonant TVA encompassing a single in vacuo composite beam is analysed with respect to measurements of the vibration transmissibility FRF taken between the displacements measured at the tips and at the centre post of the flapping beam and of the base impedance FRF taken between the force and the velocity at the centre post. Secondly, as shown in figure 4(c), the response of a multi-resonant TVA encompassing a stack of three in vacuo composite beam is analysed with respect to a measurement of the base impedance FRF taken between the force and the velocity at the base of the mast structure.

As highlighted in figures 4(a) and (b), the vibration response of a single in-vacuo composite beam held in the middle by the base post is characterized by a fundamental flapping bending vibration mode [85], whose dynamic response can be suitably modelled in terms of a resonator formed by a seismic mass and a base mass connected via a spring and a damper [86]. The seismic mass and the spring and damper represent the modal mass, modal stiffness and modal damping of the fundamental flapping vibration mode of the in-vacuo composite beam. The base mass accounts for the mass of the base junction element. As discussed in [86] the damping effect is primarily due to the air damping produced by the flapping vibration of the beam. Due to the high vacuum pressure exerted by the deflated skin, the core fabric of the composite beam is characterized by a solid state where the hollowed truss-like particles are tightly joined to each other. Hence, the friction damping between particles is negligible. There is material damping of the truss-like particles, which, nevertheless, is rather small too [69]. Thus overall, the damping effect arises from air damping.

As shown in figure 4(c) the vibration responses of the assemble of progressively shorter in-vacuo composite beams held in the middle by a rigid mast element are also characterized by fundamental flapping bending vibration modes having increasingly higher natural frequencies. Thus, their global vibration response can be modelled with the array of resonators shown in figure 4(d), which are formed by seismic masses connected to a common base mass via springs and dampers. The seismic masses and the springs and dampers represent the modal mass, modal stiffness and modal damping of the fundamental flapping vibration modes of the three in-vacuo composite beams. Here, the base mass accounts for the mass of the three junction elements that form the mast structure. To validate the models proposed in figure 4 for the vibration response of the single-resonant or multi-resonant (i.e. single beam or multi-beam) vibration absorbers, the following two subsections present measurements of the vibration transmissibility and base impedance FRFs taken by arranging the absorbers on a vibrating table as shown in figure 1.

3.1. Single TVA vibration transmissibility FRF

To start with, the dynamic response of the single-resonant TVA is investigated with reference to measurements of the vibration transmissibility FRFs given by the ratio between the complex amplitudes of the displacements at the tips and at the base of the composite beam as depicted in figure 4(a): $T_1(\omega) = w_{t1}(\omega)/w_b(\omega)$ and $T_2(\omega) = w_{t2}(\omega)/w_b(\omega)$. Here $w_{t1}(\omega)$, $w_{t2}(\omega)$, $w_b(\omega)$ are the complex amplitudes of the tip and base displacements defined assuming $e^{j\omega t}$ time dependence, where ω is the circular frequency and $j = \sqrt{-1}$. Figure 5 shows the two FRFs with respect to incremental levels of vacuum comprised between 5 and 80 kPa when the length of the composite beam is chosen in such a way as the TVA works in the vicinity of the resonance frequency of the first

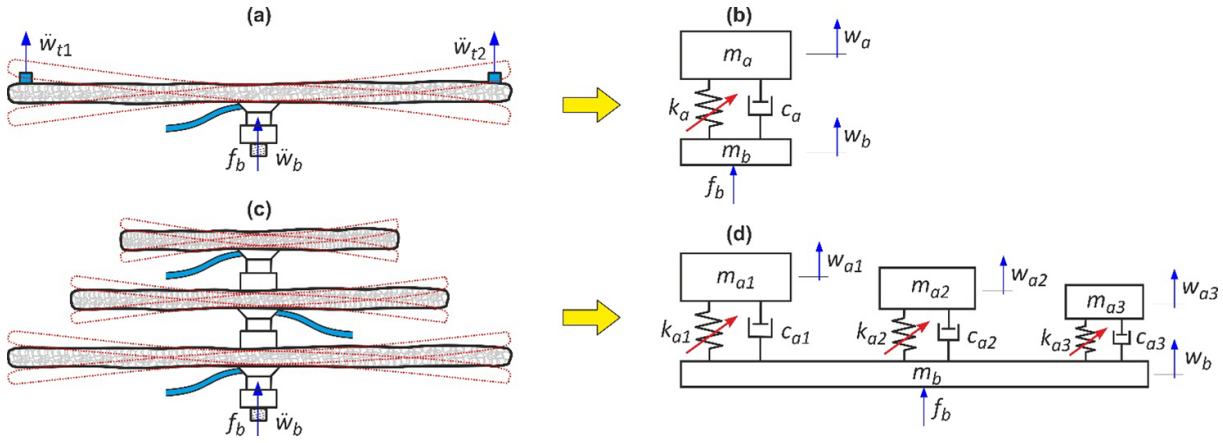

Figure 4. Flapping vibration mode (a), (c) and lumped parameter model (b), (d) of the TVA formed by a single (a), (b) and three (c), (d) deflated composite beams with core structured fabrics.

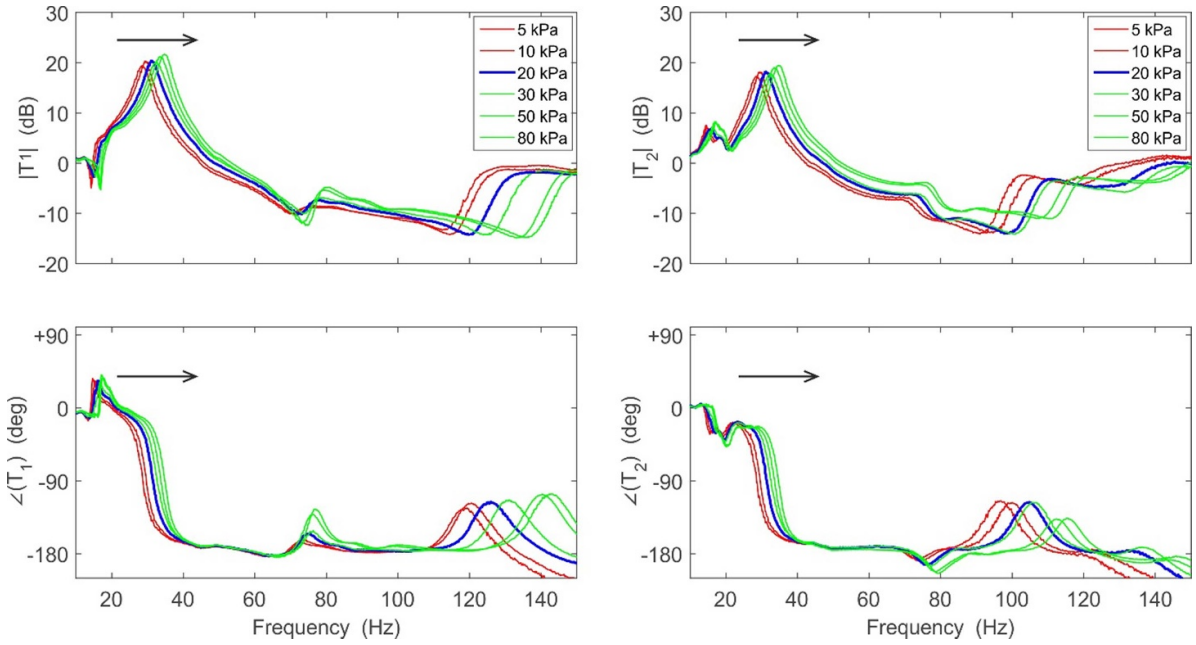

Figure 5. Measurements of the left-hand side T_1 and right-hand side T_2 vibration transmissibility FRFs taken between the displacement at the tips of the composite beam and the base displacement for the TVA tuned at about 31.7 Hz. Blue lines, optimally tuned TVA, red-lines under-tuned TVA, green lines over-tuned TVA. Arrows indicate rising vacuum pressure.

flexural mode of the plate model structure used to assess the control performance of the absorber, i.e. 31.7 Hz. At low frequencies below 100 Hz, the spectra of the two transmissibility FRFs are quite similar, which indicates that the two flapping arms vibrate evenly. There is just a small uneven resonance peak at around 5 Hz, which is probably linked to a torsional vibration of the beam. At high frequencies above 100 Hz, the two spectra show similar features although they do not overlap perfectly. Nevertheless, here the amplitude of the transmissibility functions is well below 0 dB, i.e. below 1, which indicates that the absorber does not produce significant effects.

Overall, the two spectra resemble those of the classical TVAs shown in figure 4(b) with the seismic mass and spring given by the modal mass and modal stiffness of the flapping vibration of the composite beam. In fact, at low frequencies they tend to a 0 dB amplitude asymptote with phase equal to 0 deg. Hence, for $\omega \to 0$ $|T_1(\omega)| = |T_2(\omega)|$, which indicates that the base and seismic masses vibrate together as if they were a rigid body. Then, around 31.7 Hz, they show a marked resonance peak with phase about -90 deg, which indicates the seismic mass vibrates significantly more than the base mass, such that vibration energy is absorbed from the base and dissipated by the damper. At higher frequencies, the amplitude of the transmissibility falls below 0 dB (i.e. below 1) with phase -180 deg. Here the vibration of the seismic mass is progressively smaller than that of the base mass and there is no more vibration absorption. In a way, at high frequencies,

the flapping vibration of the composite beam is characterized by fixed tips and a moving centre post. The spectra of the $T_1(\omega)$ and $T_2(\omega)$ FRFs depicted in figure 5 with colour lines indicate that, when the vacuum level in the deflated composite beam is raised from 5 kPa to 80 kPa, the frequency of the resonance peak, that is the fundamental resonance frequency of the absorber, shifts from 27 Hz to 35 Hz. Here the blue line represents the FRF for the absorber optimally tuned to control the fundamental resonant mode of the plate used to test its vibration control performance. Instead the red and green lines represent the FRFs when the absorber is respectively under-tuned or over-tuned.

3.2. Single TVA base impedance FRF

To follow, the dynamic response of the single-resonance TVAs is investigated with reference to a measurements of the base impedance FRFs given by the ratio between the complex amplitudes of the base force and velocity as depicted in figure 4(a): $Z(\omega) = f_b(\omega)/\dot{w}_b(\omega)$. Here $f_b(\omega)$ and $\dot{w}_b(\omega)$ are the complex amplitudes of the force and velocity at the base of the absorber. The graphs in figure 6, show the FRFs with respect to incremental levels of vacuum comprised between 5 and 80 kPa when the length of the composite beam is chosen in such a way as the TVA works in the vicinity of the resonance frequency of the first, second and fourth flexural mode of the plate model structure used to assess the control performance of the absorber, i.e. at 31.7 Hz, 48.6 Hz and 89.5 Hz (the third flexural mode that resonates at 84.3 Hz contributes little to the global response of the plate and thus was not controlled).

Considering first the base impedance for the TVA set to control the resonant response of the first mode shown in figure 6(a), the spectrum is characterized by a low-frequency asymptote with amplitude that rises at a rate of 20 dB/decade with phase +90 deg. There is then a resonance peak at about 31.7 Hz with a phase drop of about −180 deg, which is followed by a band where the amplitude falls at a 20 dB/-decade rate. Then, at about 42 Hz there is an anti-resonance trough with a phase recovery of about +180 deg followed by a high frequencies asymptote with 20 dB/decade rising amplitude and phase +90 deg. According to the theory of mechanical mobility and impedance functions [88], these features of the spectra indicate that at low frequencies the structured fabric absorber responds as a lumped mass given by the base and composite beam masses. There is then a resonance effect where the absorber works as a damper that dissipates the vibration energy absorbed from the vibrating base. At higher frequencies the absorber works as a spring that reacts off the seismic mass offered by the flapping vibration of the composite structure. Finally, above the anti-resonance frequency it resumes the lumped mass behaviour, although, here, the mass is given by the base component only since the flapping vibration of the composite beam is progressively much smaller than that of the base junction. The multiple spectra depicted in the graphs of figure 6(a) show that the frequency of the resonance peak where the absorber operates as a damper that efficiently absorbs and dissipates vibration energy can be suitably shifted

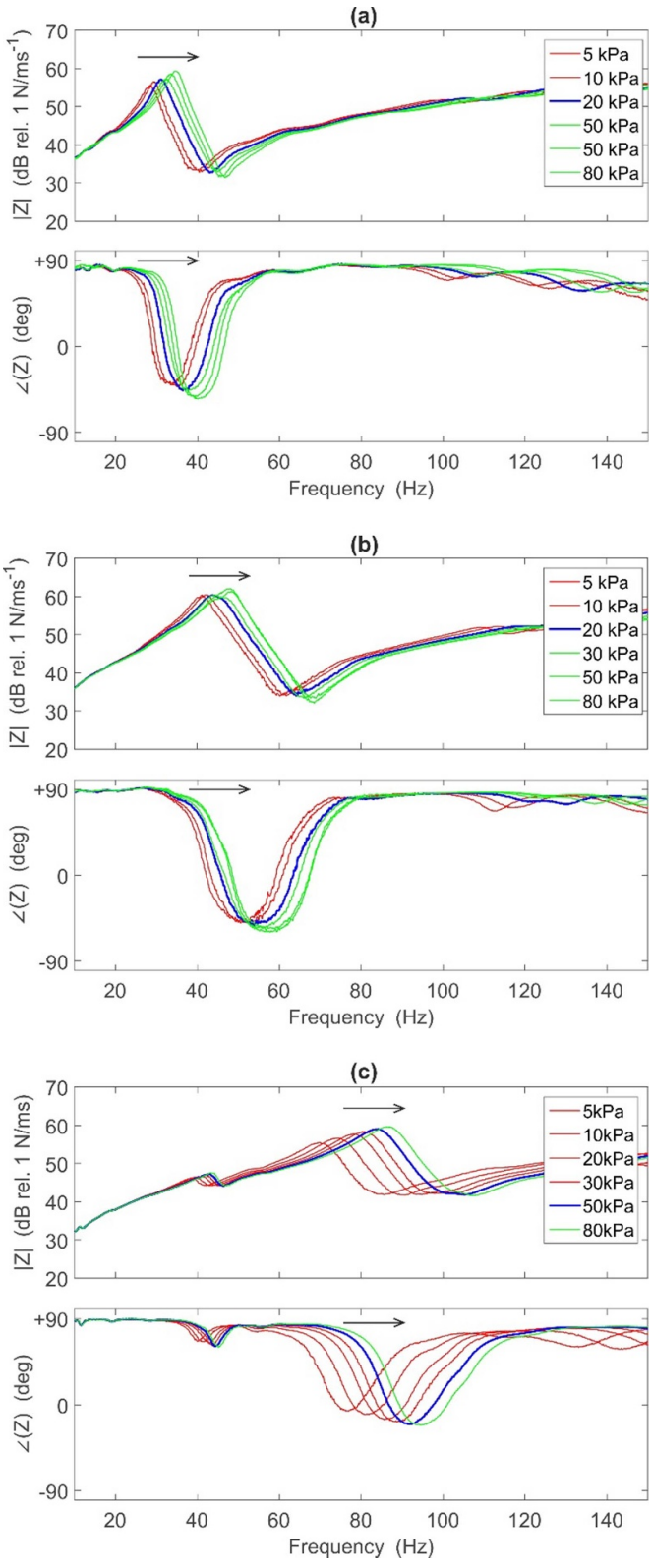

Figure 6. Measurements of the base impedance FRF for the TVA tuned around (a) 31.7 Hz, (b) 48.6 Hz, (c) 89.5 Hz. Blue line optimally tuned TVA, red lines under-tuned TVA, green lines over-tuned TVA. Arrows indicate rising vacuum pressure.

by about 7 Hz, i.e. between 27 and 35 Hz, when the vacuum pressure in the composite beam is modulated between 5 kPa and 80 kPa. The base impedance for the single-resonance

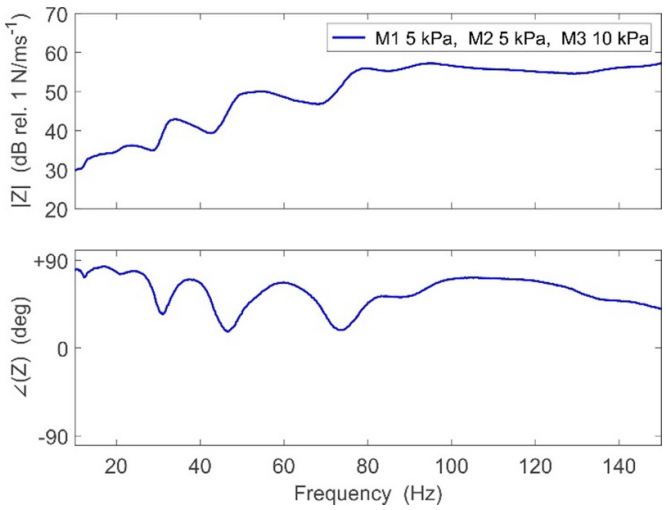

Figure 7. Measurements of the base impedance FRF for the multi-resonant TVA tuned at 31.7 Hz, 48.6 Hz, 89.5 Hz.

TVAs set to control the resonant responses of the second and fourth mode shown in figures 6(b) and (c) display the same features described for the base impedance of the single-resonance TVAs set to control the resonant response of the first mode.

Overall, the spectra of the vibration transmissibility and base impedance FRFs measured on the single-resonant TVA (figure 4(a)) show the typical feature of classical base mas-spring-damper-seismic mass absorbers (figure 4(b)). The proposed absorber can thus be suitably used to control a resonant response of the hosting structure. In particular, its fundamental resonance effect can be modulated by varying the level of vacuum in the composite structure such that it can be adapted online to maximise the vibration absorption from mechanical systems characterised by significant changes of their resonant responses, that is of their resonance frequency. It should be highlighted here that, as indicated in [69, 86], the tuning bandwidth of the absorber can be suitably expanded by playing with the number of fabrics piled into the vacuum bags, with the type (e.g. cubes, octahedral, etc) and the size (overall and of the truss elements) of the particles and with the material properties of the chain mails.

3.3. Multi TVA base impedance

To conclude, the dynamic response of the multi-resonant TVA is examined considering the spectrum of the measured base impedance FRF given by the ratio between the complex amplitudes of the base force and velocity as depicted in figure 4(c): $Z(\omega) = f_b(\omega)/\dot{w}_b(\omega)$. Here, figure 7 shows the FRF measured with the three optimally tuned composite beams having increasingly shorter lengths in such a way as the TVA works in the vicinity of the resonance frequency of the first, second and fourth flexural mode of the hosting plate structure used to assess the control performance of the absorber, i.e. at 31.7 Hz, 48.6 Hz and 89.5 Hz.

Overall, the FRF presents three sections that resemble the spectra found for the single-resonant TVAs set to control the modes of the hosting structure that resonate at 31.7 Hz, 48.6 Hz and 89.5 Hz. Hence the modulus shows a sequence of rising and falling amplitudes with slope $+20$ dB/decade -20 dB/decade separated by resonance peaks and antiresonance troughs. The phase starts at about $+90$ deg and then undergoes about -90 deg phase delay and about $+90$ deg phase recovery at the resonance and antiresonance frequencies. In principle, these phase shifts should be of ± 180 deg but the superposition of the dynamics of the three parallel resonators leads to smaller variations. Here, the resonance peaks and antiresonance troughs are more damped than those found with the single-resonant TVA.

4. TVA vibration control of multiple resonant responses of a plate structure

The vibration control performance of the TVA made with the deflated composite beams is now investigated. Both the single-resonant and multi-resonant configurations of the TVA are tested on the thin steel plate model structure shown in figure 8, which is clamped on a rigid frame and is excited in bending by a white noise point force. As discussed above, the single-resonant and multi-resonant TVAs have been equipped with deflated composite beams of increasingly smaller length such that they can be tuned around the nominal resonance frequencies of the first, second and fourth flexural mode at 31.7 Hz, 48.6 Hz and 89.5 Hz. As anticipated above, the third flexural mode that resonates at 84.3 Hz contributes little to the global response of the plate and thus was not controlled.

The global flexural response of the panel has been assessed with respect to the time-averaged flexural kinetic energy of the plate, which has been calculated from measurements of mobility FRFs taken with a laser vibrometer at a grid of points

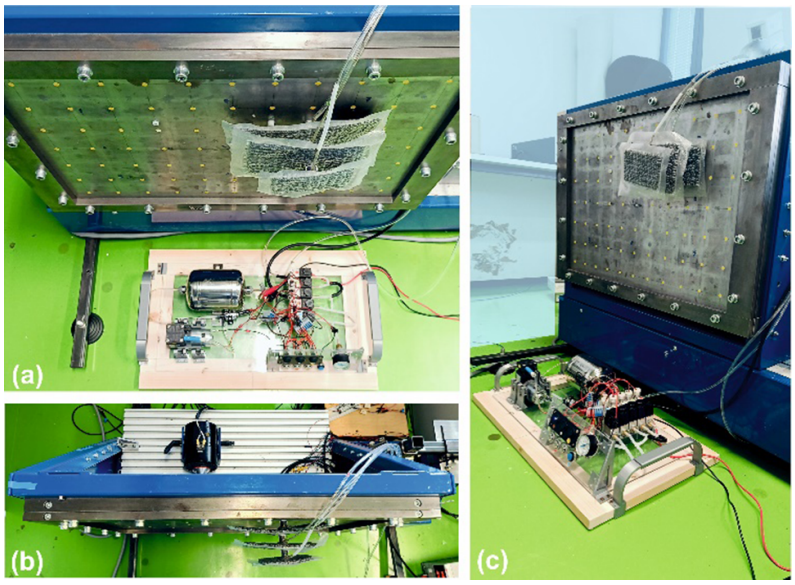

Figure 8. Plate model structure (a), (c), which is excited by a shaker (b) and is equipped with the multi-resonant vibration absorber made by three deflated composite beams (a), (c) whose pressure is controlled by the vacuum plant (a), (c).

with respect to the force excitation. Hence the time-averaged flexural vibration energy has been derived with the following formula [86]:

$$K(\omega) = \frac{M}{4}\sum_{\mathrm{n}=1}^{\mathrm{N}} |Y_{\mathrm{n}}(\omega)|^2 F^2, \tag{2}$$

where $Y_n(\omega)$ are the mobility functions [88] measured with the laser vibrometer at a regular grid of $N = 6 \times 4 = 24$ points, F is the amplitude of the force excitation and M is the mass of the plate.

4.1. Single-resonant TVA

Figures 9(a), 10(a), 11(a) show the 10–150 Hz spectra of the time-averaged flexural kinetic energy per unit force excitation of the plain panel (solid black line) and of the panel with single-resonant TVAs having composite beam lengths set to control in turn the resonant responses due to the first, second and forth natural modes (solid blue line). Also, figures 9(b), 10(b), 11(b) show frequency zooms of the spectra when the TVA with the deflated composite beam is under-tuned (red lines), optimally tuned (blue line) and over-tuned (green lines).

The spectrum of the response for the plain panel is characterized by 6 sharp peaks at 31.7 Hz, 48.6 Hz, 84.3 Hz, 89.5 Hz, 109.6 Hz, 132.9 Hz, which are controlled by the resonant responses of the first six natural modes of the panel. The third peak at 84.3 Hz is significantly smaller than the others and thus both the single-resonant and multi-resonant TVAs have been tuned to control only the resonant responses of the first, second and fourth modes of the panel. Figures 9(a), 10(a), 11(a) show that, when the plate is equipped with the optimally tuned single-resonant TVAs, the spectrum is modified at the resonance frequency of the target mode with a double peak having attenuated amplitude. More specifically, the amplitude of the first, second and fourth resonance peaks are reduced by about 14 dB, 20 dB, 11 dB respectively. As one would expect, the kinetic energy spectra for the panel with the optimally tuned absorbers are characterized by a small double peak. As discussed in Section 2.2, the flapping vibration of the deflated composite beam is characterised by about 20% damping ratio, which is about optimal to maximize the vibration dissipation in the TVA, that is the vibration absorption by the TVA. To conclude, the zooms in figures 9(b), 10(b), 11(b) show that the level of vacuum can be suitably used to finely tune the TVAs to control the resonant responses of the target modes.

4.2. Multi-resonant TVA

Figure 12 shows the 10–150 Hz spectrum of the time-averaged flexural kinetic energy per unit force excitation of the plain panel (solid black line) and of the panel with the multi-resonant TVA, which, as shown in figure 1, incorporates three increasingly shorter composite beams whose lengths have been set to control simultaneously the resonant responses due to the first, second and forth flexural modes of the panel (solid blue line). Figure 13 shows the same graph but with the multi-resonant TVA under-tuned (red lines), optimally tuned (blue line) and over-tuned (green lines). Figure 12 shows that, indeed, the multi-resonant TVA effectively controls the resonant responses of the target modes. More specifically the amplitudes of the first, second and fourth resonance peaks at 31.7 Hz, 48.6 Hz, 89.5 Hz are brought down by 18, 19, 18 dB. The graph shows that the higher frequency dynamics of the absorber generates 5 and 8 dB reductions of the fifth and sixth resonance peaks at 109.6 Hz and 132.9 Hz.

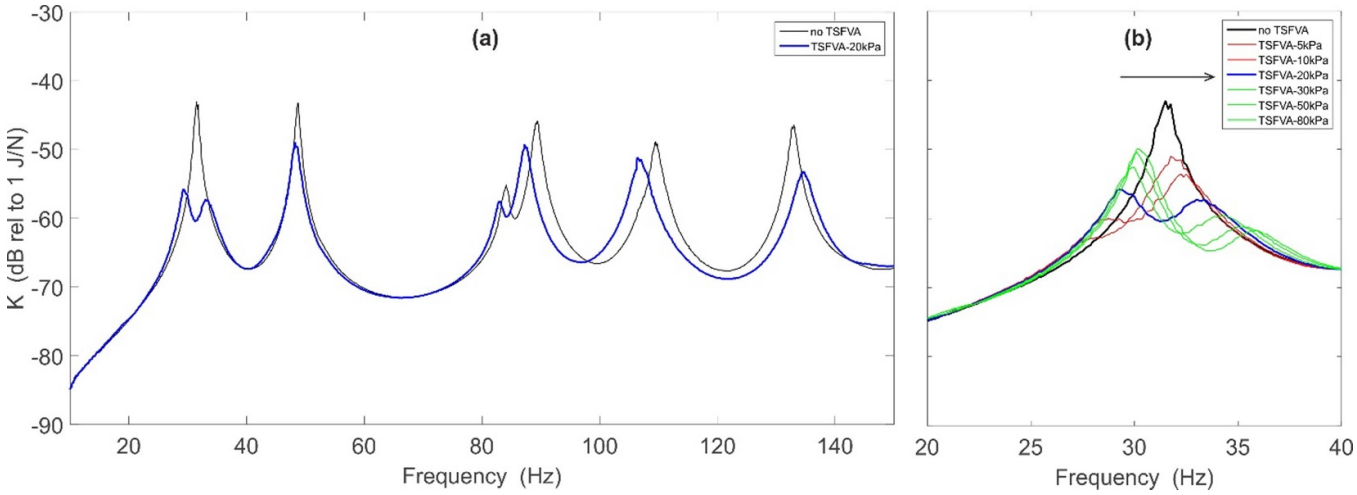

Figure 9. Measured spectra of the time-averaged flexural kinetic energy of the panel per unit force excitation. (a) Plain panel (black line) and panel with TVA tuned to control the resonant response of mode N. 1 (blue line). (b) Zoom with TVA under-tuned (red lines), optimally tuned (blue line) and over-tuned (green lines). Arrow indicates rising vacuum pressure.

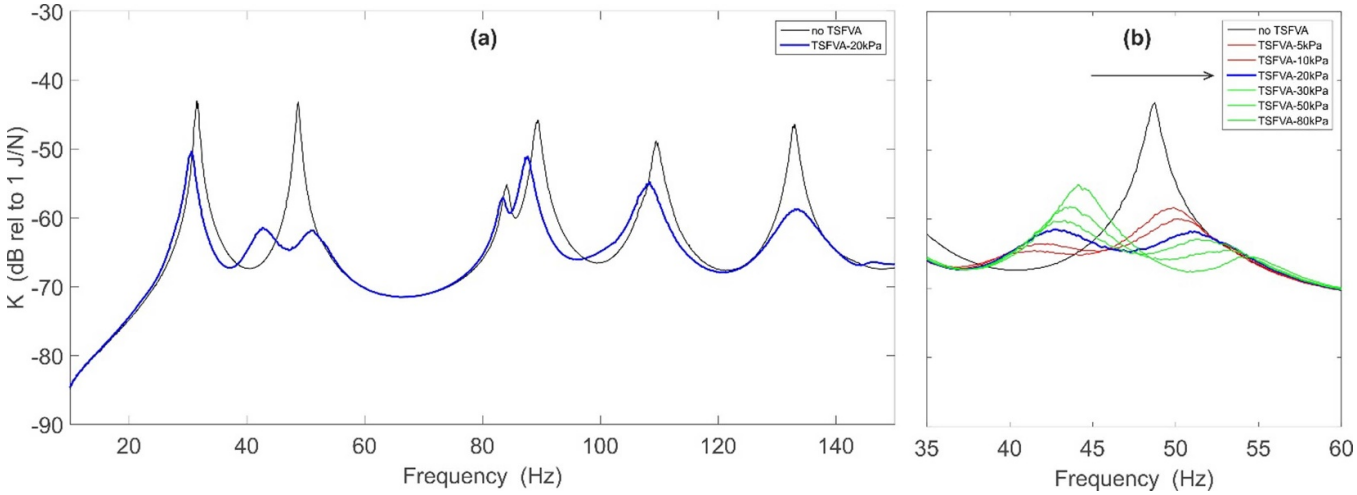

Figure 10. Measured spectra of the time-averaged flexural kinetic energy of the panel per unit force excitation. (a) Plain panel (black line) and panel with TVA tuned to control the resonant response of mode N. 2 (blue line). (b) Zoom with TVA under-tuned (red lines), optimally tuned (blue line) and over-tuned (green lines). Arrow indicates rising vacuum pressure.

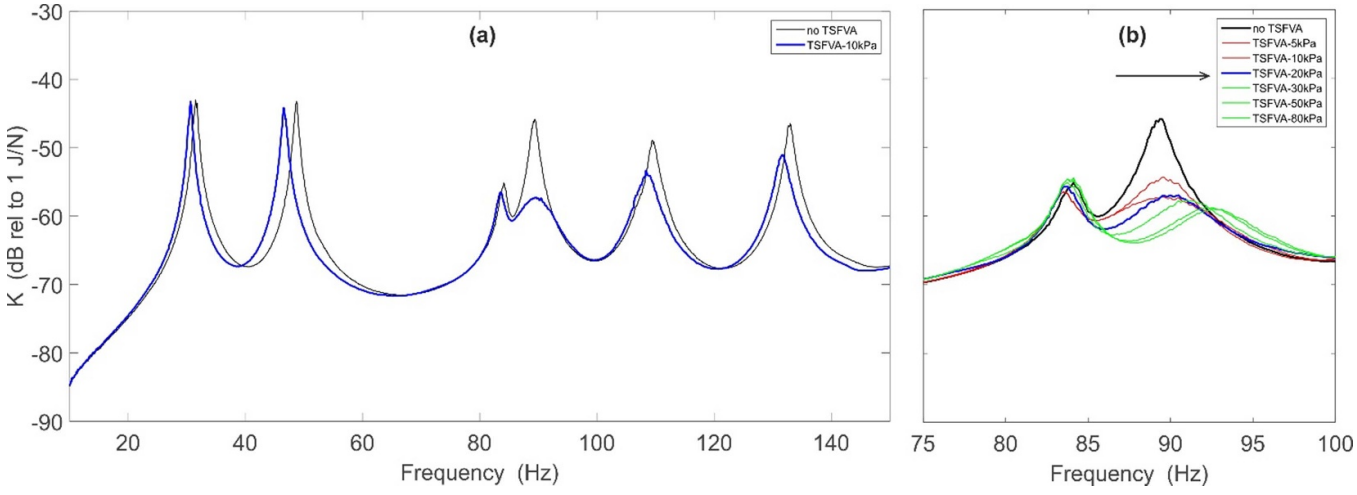

Figure 11. Measured spectra of the time-averaged flexural kinetic energy of the panel per unit force excitation. (a) Plain panel (black line) and panel with TVA tuned to control the resonant response of mode N. 4 (blue line). (b) Zoom with TVA under-tuned (red lines), optimally tuned (blue line) and over-tuned (green lines). Arrow indicates rising vacuum pressure.

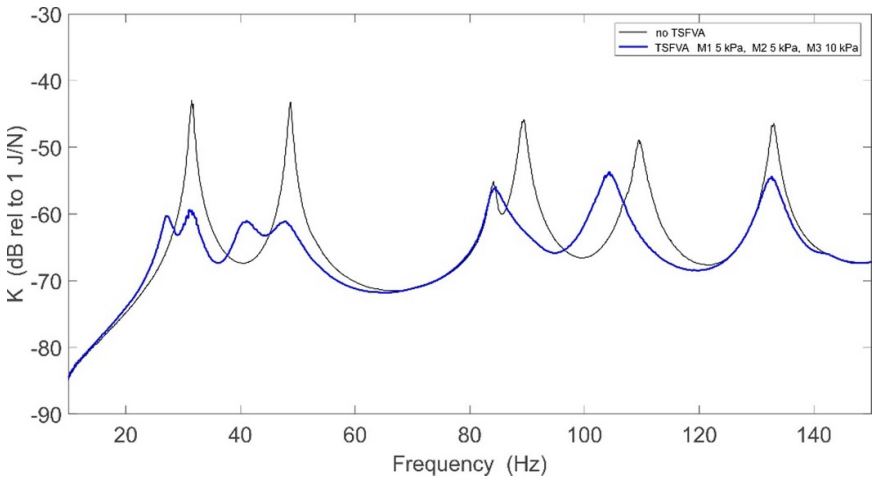

Figure 12. Measured spectra of the time-averaged flexural kinetic energy of the panel per unit force excitation. (a) Plain panel (black line) and panel with TVA tuned to control the resonant response of modes N. 1, 2, 4 (blue line).

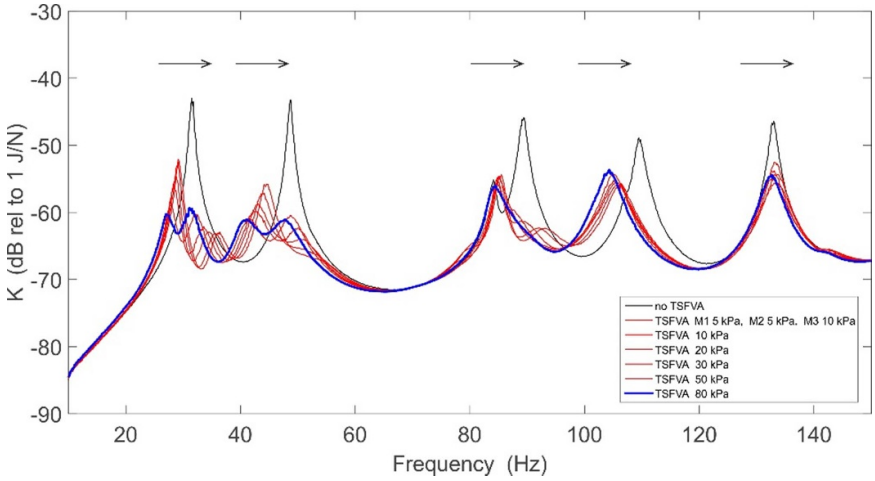

Figure 13. Measured spectra of the time-averaged flexural kinetic energy of the panel per unit force excitation. (a) Plain panel (black line) and panel with TVA under-tuned and over-tuned (red lines). Arrows indicate rising vacuum pressure.

Figure 13 shows how the vacuum pressure of the three composite beams influences the multi-resonant tuning of the absorber. The graph highlights the typical phenomenon where the under-tuned absorber generates a higher-left and lower-right pair of peaks whereas the over-tuned absorber generates a lower-left and higher-right pair of peaks. As for classical single-resonance TVA, the optimal tuning generates equal amplitude resonance peaks.

5. Conclusions

This paper has presented a new multi-resonant vibration absorber formed by a tree of deflated composite beams fixed in the middle to a mast structure. Each beam is formed by a core structured fabric wrapped on an outer plastic skin, which is deflated. The vacuum level is used to tune the resonance frequency of the flapping vibration mode of each beam, which generates the vibration absorption effect.

The paper shows that the natural frequencies of the composite beams can be suitably shifted over a range of about 8 Hz. Thus, provided the length of the composite beams are selected in such a way that they resonate at the nominal resonance frequencies of the target modes of the hosting structure, they can be tuned online to track changes in the dynamic response of both the hosting structure and TVA itself due to production variability, to wearing over time and to changes during operation generated for example by changes of temperature or fluctuations of imposed loads. The study has considered both single-resonant and multi-resonant configurations of the absorber mounted on a thin plate model structure. When the single-resonant vibration absorber is tuned to control in turn the first, second and fourth modes of the hosting plate structure, the amplitude of the first, second and fourth resonance peaks in the spectrum of the plate flexural response are attenuated by about 14 dB, 20 dB, 11 dB respectively. Alternatively, when the multi-resonant vibration absorber is tuned to control simultaneously the first, second and fourth modes of the hosting plate structure, the amplitude of the first, second and fourth

resonance peaks are attenuated by about 18 dB, 19 dB, 18 dB respectively.

It is expected that the proposed absorber made with 'deflatable' composite beams can be developed into a self-tuning absorber where the vacuum level is controlled online in such a way as to maximize the vibration absorption. This can be suitably done by measuring the vibration power absorption at the base of the absorber with an impedance head. In this case, the self-tuning can be implemented with a model free extremum seeking algorithm for example.

Data availability statement

All data that support the findings of this study are included within the article (and any supplementary files).

Acknowledgment

This work was funded by the European Union under NextGenerationEU. PRIN 2022 Prot. n. 20223X5S37_001.

ORCID iDs

Paolo Gardonio https://orcid.org/0000-0001-5366-4239
Lisa Ortis https://orcid.org/0009-0001-5604-2133
Emiliano Rustighi https://orcid.org/0000-0001-9871-7795
Ciro Malacarne https://orcid.org/0000-0003-4032-1813
Matteo Perini https://orcid.org/0000-0002-6099-0419

References

[1] Fahy F and Gardonio P 2007 *Sound and Structural Vibration* (Academic)
[2] Langley R S and Fahy F J 2004 High-frequency structural vibration *Applications in Acoustics, Noise and Vibration* ed F Fahy and J Walker (CRC Press) pp 490–529
[3] Gardonio P and Turco E 2019 Tuning of vibration absorbers and Helmholtz resonators based on modal density/overlap parameters of distributed mechanical and acoustic systems *J. Sound Vib.* **451** 32–70
[4] Thompson D 2015 Noise Control *Fundamentals of Sound and Vibration* ed F Fahy and D Thompson (CRC Press) pp 213–310
[5] Arenas J P and Crocker M J 2010 Recent trends in porous sound-absorbing materials *J. Sound Vib.* **44** 12–17
[6] Brennan M and Walker J 2004 *Advanced Applications in Acoustics, Noise and Vibration* ed F Fahy and J Walker (CRC Press) pp 530–80
[7] Fuller C R, Elliott S J and Nelson P A 1996 *Active Control of Vibration* (Academic)
[8] Clark R L, Saunders W R and Gibbs G P 1998 *Adaptive Structures* 1st edn (Wiley)
[9] Elliott S J 2000 *Signal Processing for Active Control* (Academic)
[10] Moheimani S O R and Fleming A J 2006 *Piezoelectric Transducers for Vibration Control and Damping* (Springer)
[11] Hansen C, Snyder S, Qiu X, Brooks L and Moreau D 2012 *Active Control of Noise and Vibration* (CRC Press)
[12] Preumont A 2018 *Vibration Control of Active Structures* (Springer)
[13] Gardonio P 2002 Review of active techniques for aerospace vibro-acoustic control *J. Aircr.* **39** 206–14
[14] Elliott S J 2008 A review of active noise and vibration control in road vehicles *ISVR Tech. Memorandum No 981*
[15] Gardonio P 2010 *Active Noise Control 293 in Encyclopedia of Aerospace Engineering* ed R Blockley and W Shyy (Wiley)
[16] Frahm H 1911 Device for damping vibrations of bodies Patent US989958A (USA)
[17] Ormondroyd J D and Hartog J P 1928 The theory of the dynamic vibration absorber *J. Appl. Mech.* **50** 9–22
[18] Brock J E 1946 A note on the damped vibration absorber *J. Appl. Mech.* **3** A284
[19] Den Hartog J P 1956 *Mechanical Vibrations* 4th edn (McGraw-Hill)
[20] Hunt J B 1979 *Dynamic Vibration Absorbers* vol 117 (Mechanical Engineering Publications Limited)
[21] Inman D J 1994 *Engineering Vibration* vol 621 (Prentice-Hall)
[22] Mead D J 2000 *Passive Vibration Control* (Wiley)
[23] Gardonio P, Turco E, Kras A, Dal Bo L and Casagrande D 2021 Semi-active vibration control unit tuned to maximise electric power dissipation *J. Sound Vib.* **499** 116000
[24] Crandall S H and Mark W D 1963 *Random Vibration in Mechanical Systems* (Academic) pp 371–2
[25] Iwata Y 1982 On the construction of the dynamic vibration absorber *Jpn. Soc. Mech. Eng.* **820** 150–2
[26] Sun J Q, Jolly M R and Norris M A 1995 Passive, adaptive and active tuned vibration absorbers-a survey *J. Vib. Acoust.* **117** 234–42
[27] Nishihara O and Asami T 2002 Closed-form solutions to the exact optimizations of dynamic vibration absorbers (minimizations of the maximum amplitude magnification factors) *J. Vib. Acoust.* **124** 576–82
[28] Krenk S 2005 Frequency analysis of the tuned mass damper *J. Appl. Mech.* **72** 936–42
[29] Bisegna P and Caruso G 2012 Closed-form formulas for the optimal pole-based design of tuned mass dampers *J. Sound Vib.* **331** 2291–314
[30] Krenk S and Høgsberg J 2012 Equal modal damping design for a family of resonant vibration control formats *J. Vib. Control* **19** 1294–315
[31] Zilletti M, Elliott S J and Rustighi E 2012 Optimisation of dynamic vibration absorbers to minimise kinetic energy and maximise internal power dissipation *J. Sound Vib.* **331** 4093–100
[32] Warburton G B 1982 Optimum absorber parameters for various combinations of response and excitation parameters Earthquake *Eng. Struct. Dyn.* **10** 381–401
[33] Krenk S and Høgsberg J 2008 Tuned mass absorbers on damped structures under random load *Probabilistic Eng. Mech.* **23** 408–15
[34] Krenk S and Høgsberg J 2014 Tuned mass absorber on a flexible structure *J. Sound Vib.* **333** 1577–95
[35] Krenk S and Høgsberg J 2016 Tuned resonant mass or inerter-based absorbers: unified calibration with quasi-dynamic flexibility and inertia correction *Proc. R. Soc.* A **472** 20150718
[36] Snowdon J C, Wolfe A A and Kerlin R L 1964 The cruciform dynamic vibration absorber *J. Acoust. Soc. Am.* **75** 1792–9
[37] Jolly M R and Sun J Q 1996 Passive tuned vibration absorbers for sound radiation reduction from vibrating panels *J. Sound Vib.* **191** 577–83
[38] Zuo L and Nayfeh S A 2004 Minimax optimization of multi-degree-of-freedom tuned-mass dampers *J. Sound Vib.* **272** 893–908
[39] Gardonio P and Zilletti M 2013 Integrated tuned vibration absorbers: a theoretical study *J. Acoust. Soc. Am.* **134** 3631–44
[40] Holdhusen M H and Cunefare K A 2007 A state-switched absorber used for vibration control of continuous systems *J. Vib. Acoust.* **129** 577–89

[41] Guyomar D, Richard C and Mohammadi S 2007 Semi-passive random vibration control based on statistic *J. Sound Vib.* **307** 818–33

[42] Gardonio P and Zilletti M 2015 Sweeping tuneable vibration absorbers for low-mid frequencies vibration control *J. Sound Vib.* **354** 1–12

[43] Von Flotow A H, Beard A and Bailey D 1994 Adaptive tuned vibration absorbers: tuning laws, tracking agility, sizing, and physical implementation *Proc. Noise-Con 94 (Ft. Lauderdale, Florida)* pp 437–54

[44] Charette F, Fuller C and Carneal L 1997 Adaptive vibration absorbers for control of sound radiation from panels *AIAA-97-1619-C*

[45] Von Flotow A, Mercadal M, Maggi L and Adams N 1997 Vibration and sound in aircraft cabins; a comparison of adaptive/passive and active control *SAE Conf.* (*Wichita, Kansan*)

[46] Huang Y and Fuller C R 1997 The effects of dynamic absorbers on the forced vibration of a cylindrical shell and its coupled interior sound field *J. Sound Vib.* **300** 401–18

[47] Brennan M J 1997 Vibration control using a tunable vibration neutralizer *Proc. Inst. Mech. Eng.* C **211** 91–108

[48] Howard C 2009 Review of adaptive tuned vibration neutralisers *Proc. Acoust* (*Adelaide, Australia*, *23–25 November 2009*)

[49] Rustighi E, Ledezma-Ramirez D F, Tapia-Gonzalez P E, Ferguson N and Zakaria A 2021 Modelling and experimental characterisation of a compressional adaptive magnetorheological elastomer isolator *J. Vib. Cont.* **28** 3093–107

[50] Kumbhar S B, Chavan S P and Gawade S S 2018 Adaptive tuned vibration absorber based on magnetorheological elastomer-shape memory alloy composite *Mech. Syst. Signal Process.* **100** 208–23

[51] Rustighi E, Brennan M J and Mace B R 2004 A shape memory alloy adaptive tuned vibration absorber: design and implementation *Smart Mater. Struct.* **14** 19–28

[52] Manzoni S, Argentino A, Lucà F, Berardengo M and Vanali M 2023 SMA-based adaptive tuned mass dampers: analysis and comparison *Mech. Syst. Signal Process.* **186** 109883

[53] Bonello P, Brennan M J, Elliott S J, Vincent J F V and Jeronimidis G 2005 Designs for an adaptive tuned vibration absorber with variable shape stiffness element *Proc. R. Soc.* A **461** 3955–76

[54] Behrens S, Fleming A J and Moheimani S O R 2005 Passive vibration control via electromagnetic shunt damping *IEEE/ASME Trans. Mechatronics* **10** 118–22

[55] McDaid A J and Mace B R 2016 A self-tuning electromagnetic vibration absorber with adaptive shunt electronics *Smart Mater. Struct.* **22** 105013

[56] Turco E and Gardonio P 2017 Sweeping shunted electro-magnetic tuneable vibration absorber: design and implementation *J. Sound Vib.* **407** 82–105

[57] Turco E, Gardonio P, Petrella R and Bo L D 2020 Modular vibration control unit formed by an electromagnetic proof-mass transducer and sweeping resistive-inductive shunt *J. Vib. Acoust.* **142** 061005

[58] Ranchek M A, Ryan M W and Bernhard R J 1995 Adaptive passive vibration control *J. Sound Vib.* **189** 565–85

[59] Pisano M, Turco E, Petrone G, Gardonio P and De Rosa S 2023 Number vs size of electro-mechanical tuneable vibration absorbers for aeronautical applications: a case study *J. Sound Vib.* **561** 117827

[60] Alujević N, Tomac I and Gardonio P 2012 Tuneable vibration absorber using acceleration and displacement feedback *J. Sound Vib.* **331** 2713–28

[61] Zhao G, Alujević N, Depraetere B and Sas P 2015 Dynamic analysis and H2 optimisation of a piezo-based tuned vibration absorber *J. Intell. Mater. Syst. Struct.* **26** 1995–2010

[62] Hollkamp J J and Starchville T F A 1994 Self-tuning piezoelectric vibration absorber *J. Intell. Mater. Syst. Struct.* **5** 559–66

[63] Fleming A J and Moheimani S O R 2003 Adaptive piezoelectric shunt damping *Smart Mater. Struct.* **12** 36–48

[64] Niederberger D and Morari M 2006 An autonomous shunt circuit for vibration damping *Smart Mater. Struct.* **15** 359–64

[65] Gripp J A B, Góes L C S, Heuss O and Scinocca F 2015 An adaptive piezoelectric vibration absorber enhanced by a negative capacitance applied to a shell structure *Smart Mater. Struct.* **24** 15

[66] Gardonio P, Zientek M and Dal Bo L 2019 Panel with self-tuning shunted piezoelectric patches for broadband flexural vibration control *Mech. Syst. Signal Process.* **134** 106299

[67] Rodrigues G K *et al* 2022 Piezoelectric patch vibration control unit connected to a self-tuning RL-shunt set to maximise electric power absorption *J. Sound Vib.* **536** 117–54

[68] Wang Y, Li L, Hofmann D, Andrade J E and Daraio C 2021 Structured fabrics with tunable mechanical properties *Nature* **596** 238–43

[69] Rustighi E, Gardonio P, Baldini S, Malacarne C and Perini M 2024 Vibration response of in-vacuo tuneable structured fabrics *J. Vib. Control* (https://doi.org/10.1177/10775463241245251)

[70] Engel J and Liu C 2007 Creation of a metallic micromachined chain mail fabric *J. Micromech. Microeng.* **17** 551–6

[71] Wijnhovena M A and Moskvin A 2020 Digital replication and reconstruction of mail armour *J. Cult. Herit.* **45** 221–33

[72] Liu A J and Nagel S R 1998 Jamming is not just cool anymore *Nature* **396** 21–22

[73] Levine D 2001 Jamming and the statics of granular materials *Jamming and Rheology: Constrained Dynamics on Microscopic and Macroscopic Scales* (CRC Press Taylor & Francis Group) p 9

[74] Liu J and Nagel S R 2001 *Jamming and Rheology: Constrained Dynamics on Microscopic and Macroscopic Scales* (Taylor & Francis)

[75] O'Hern C S and Silbert L E 2003 Jamming at zero temperature and zero applied stress: the epitome of disorder" *Phys. Rev.* E **68** 011306

[76] Bi D, Zhang J, Chakraborty B and Behringer R P 2011 Jamming by shear *Nature* **480** 355–8

[77] Jaeger H 2015 Celebrating Soft Matter's 10th anniversary: toward jamming by design *Soft Matter* **11** 12

[78] Behringer R P and Chakraborty B 2018 The physics of jamming for granular materials: a review *Rep. Prog. Phys.* **82** 012601

[79] Dyskin A V, Estrin Y, Kanel-Belov A J and Pasternak E 2001 A new concept in design of materials and structures: assemblies of interlocked tetrahedron-shaped elements *Scr. Mater.* **44** 2689–94

[80] Dyskin A V, Pasternak E and Estrin Y 2012 Mortarless structures based on topological interlocking *Front. Struct. Civ. Eng.* **6** 188–97

[81] Jaeger H M, Nagel S R and Behringer R P 1996 The physics of granular materials *Phys. Today.* **49** 32–39

[82] Majmudar T S and Behringer R P 2005 Contact force measurements and stress-induced anisotropy in granular materials *Nature* **435** 1079–82

[83] Pazouki A, Kwarta M, Williams K, Likos W, Serban R, Jayakumar P and Negrut D 2017 Compliant contact versus rigid contact: a comparison in the context of granular dynamics *Phys. Rev.* E **96** 4
[84] Li L, Marteau E and Andrade J E 2019 Capturing the inter–particle force distribution in granular material using LS–DEM *Gran. Matter* **21** 1–16
[85] Snowdon J C and Nobile M A 1980 Beamlike dynamic vibration absorbers *Acustica* **44** 98–108
[86] Gardonio P, Rustigh E, Baldini S, Malacarne C and Perini M 2005 In-vacuo adaptive beam element for vibration control *Mech. Syst. Signal Process.* **224** 112089
[87] Blevins R D 2016 *Formulas for Dynamics, Acoustics and Vibration* (Wiley)
[88] Gardonio P and Brennan M J 2004 Mobility and impedance methods in structural dynamics *Advanced Applications in Acoustics, Noise and Vibration* ed F Fahy and J Walker (CRC Press) pp 389–447